

2.5 THz GaAs MONOLITHIC MEMBRANE-DIODE MIXER A NEW PLANAR CIRCUIT REALIZATION FOR HIGH FREQUENCY SEMICONDUCTOR COMPONENTS

Peter H. Siegel, R. Peter Smith, Michael Gaidis, Suzanne Martin, Judy Podosek, Ute Zimmermann
California Institute of Technology, Jet Propulsion Laboratory, Pasadena, CA 91109

ABSTRACT

A novel GaAs monolithic membrane-diode (MOMED) structure has been developed and implemented as a 2.5 THz Schottky diode mixer. The mesa-style planar diode uses a rectangular anode with a T-shaped metalization and a footprint that measures nominally $0.2\mu\text{m}$ by $1\mu\text{m}$. It is integrated onto a $3\mu\text{m}$ thick by $36\mu\text{m}$ wide by $600\mu\text{m}$ long GaAs membrane which bridges across an aperture in a monolithic all GaAs support frame approximately $50\mu\text{m}$ thick. RF filter structures are incorporated on the $600\mu\text{m}$ long membrane. The membrane frame and RF circuit are coupled to an electroformed waveguide mount that places the diode across the center of a 2.5 THz full height rectangular waveguide ($100\times 50\mu\text{m}^2$). The mixer mount contains an integrated Pickett-Potter feed horn and rectangular waveguide transformer, suspended-stripline single-mode RF filter channels to house the membrane, a fixed waveguide backshort for RF matching and a quartz-based transformer for the desired 7-21 GHz IF output. Measurements of receiver performance, in air, yield a T_{receiver} of 20,000 K DSB at 8.4 GHz IF using a 150K commercial Miteq amplifier. The receiver conversion loss measures 17 dB (including air, diplexer, IF filter and horn coupling losses), yielding a derived front-end noise temperature of approximately 12,500K DSB at 2514 GHz. A CO_2 -pumped methanol far-IR laser is used as a local oscillator at 2522 GHz and is injected with a Martin-Puplett diplexer. The required local oscillator power is below 3mW for optimum pumping, and no device damage was observed with incident power as high as 22mW. Improvements in noise temperature are expected as the devices and circuits are still being optimized. The mixer is baselined for flight use on the Earth Observing System Microwave Limb Sounder instrument to measure O_2 at 2502 GHz and OH at 2510 and 2514 GHz. EOS-MLS is scheduled for launch in 2002 on the Chem I platform, as part of NASA's Mission to Planet Earth.

I. INTRODUCTION

The THz frequency range offers a unique challenge for both heterodyne circuit and device designers. It represents a cross-over regime where wavelength scales stretch the tolerances of traditional machining as well as the dimensions and geometries accessible through photolithographic processes. In addition, critical device and RF circuit dimensions require submicron resolution to reduce parasitics whereas surrounding circuitry, especially at the intermediate frequencies which lie in the microwave bands, require macroscopic structures with smooth mechanical and electronic transitions to the RF environment. In this paper we report on a process and component design which blends the flexibility of mechanical machining and the tight tolerances and multiple die processing advantages of micro-machining. Although the techniques and circuit concepts described in this paper have been aimed at a specific flight component realization, a 2.5 THz Schottky diode mixer, other millimeter and submillimeter-wave GaAs semiconductor circuits can be enhanced with similar processing: frequency multipliers, detectors, oscillators, antenna coupled devices, planar array circuits, etc. The mixture of semiconductor and mechanical fabrication techniques, the blending of the active device and surrounding passive RF circuitry, the enhanced reliability and ease of handling of the planar circuit and the solid RF performance achieved with the first demonstration circuit, have opened a window of opportunity for submillimeter-wave semiconductor circuitry.

II. GaAs MEMBRANE

Ila. Introduction and Concept:

Due to moding effects, high frequency circuits are often limited by the thickness of the support substrates that must be used to define the active and passive RF structures used for signal processing. After device and circuit processing, microwave semiconductor substrates are generally mechanically lapped to a thickness as small as 50 microns; but even 50 microns is too thick for microstrip cir-

cuits above 300 GHz. Also, III-V semiconductors like GaAs are extremely brittle, and handling is a major problem with these wafer dimensions. Wet chemical etching has been used to thin GaAs-based devices to a thickness of <5 microns, but here again, handling and cracking of the substrate material becomes a major concern.

Silicon micromachining techniques have been used very successfully to make a variety of RF structures and components, including superconducting mixers, with dimensions compatible with THz circuitry [1-6]. However, these components rely on the mechanical, not the electrical properties of the silicon for their applications. At high frequencies, silicon cannot be used to form good quality active devices, i.e., diodes, transistors, etc. For device applications above 50 GHz, III-V semiconductors, especially GaAs, are preferred over silicon. Several research groups [7-10] have recently investigated GaAs membrane structures. These approaches have led to techniques for fabricating GaAs membranes of multiple shapes and sizes for a few assorted mechanical applications. Although some device incorporation has been attempted [8, 11], no one has yet taken advantage of the combined device/RF properties afforded by a GaAs membrane technology, nor realized a membrane fabrication approach that is compatible with existing high frequency circuits and devices.

The GaAs membrane process we have developed is tailored specifically for compatibility with existing RF circuit and two terminal device realizations at THz frequencies. It is a relatively straightforward process, requires no strongly anisotropic etchants, makes use of a simple epitaxial layer structure with two AlGaAs etch stops and is directly compatible with our existing THz planar diode fabrication process [12].

IIb. Diode and Membrane Fabrication:

The 2.5 THz mesa air-bridge T-anode Schottky barrier diodes used for the mixer circuit described in this paper are fabricated in a process which is similar to one we developed for THz resonant tunneling diodes [13] with a few enhancements and a novel planarization step. In order to allow subsequent membrane formation the GaAs host wafer has the epitaxial structure shown in Fig. 1. The only additional layer structure required over our traditional mesa Schottky diodes are the 3 μ m thick semi-insulating layer and the lower etch stop which define the membrane. All device and surrounding RF circuit processes are completed before membrane definition occurs.

For the 2.5 THz diode definition, the wafer structure consists of a thin (<1000 Å), $10^{18}/\text{cm}^3$ n-type Schottky layer, a heavily doped (5×10^{18}), one micron thick n+ layer for low-resistance ohmic contact and a thin (≈ 600 Å) AlGaAs etch stop layer. Front-side lithography is defined using a combination of tools including a 5x I-line projection mask aligner, a 50 kV electron beam system, and contact lithography. Conventional recessed Au/Ge/Ni/Ag/Au ohmic contacts are used. Two mesas are required for each device because of our anode process [13]. The active mesa is only about a micron larger than the ohmic contact, and it is etched using a selective $\text{BCl}_3/\text{SF}_6/\text{Ar}$ mixture in an electron cyclotron resonance (ECR) reactive ion-etch system (RIE). Mesa edges and the etched field are smooth. A subsequent metalization step is used to provide air-bridges to the tops of the vertical mesa walls and to form the RF filters and the IF and DC bias lines used to connect the diode with off-chip mixer circuitry.

Anodes are formed using a novel PMMA quasi-planarization technique followed by a PMMA/copolymer/PMMA trilayer resist as is commonly used for HEMT or FET T-gates [13]. The PMMA planarization is done by spinning on multiple layers of 495k PMMA to a thickness of approximately 4 to 5 microns, much thicker than the height of the mesas, followed by a sequence of deep-UV blanket exposures and brief acetone spin-develop steps until the mesa tops are exposed. PMMA was chosen for the planarization because more commonly used substances turned out to be incompatible with the PMMA used for the anode lithography. The definition of the Ti/Pt/Au anodes has been described elsewhere [14]. Finally, plasma enhanced chemical vapor deposition (PECVD) silicon nitride is used to passivate the finished devices.

The first membrane-related processing step lithographically defines the membrane strips from the topside of the wafer. CF_4/O_2 RIE is used to remove the silicon nitride device passivation layer. An ECR system using BCl_3/Ar , then $\text{BCl}_3/\text{SF}_6/\text{Ar}$, is used to continue etching down to the lower AlGaAs etch stop layer. Material must be left wherever the membranes themselves are to be formed as well as over the tops of the frames so that there is no step incurred for the metallization layer as it traverses the frame.

The wafer is next mounted topside-down, using wax, onto a suitable carrier wafer, e.g. silicon,

glass or sapphire. The backside is then lapped and polished to the desired frame thickness of 50 μm . After lapping, the backside of the wafer is cleaned by subjecting it to a light etch and then protected by a low temperature deposited (ECR) silicon nitride layer. The back of the wafer is then coated with photoresist and, employing a backside aligner, the relative positioning of the membrane and support frame is accomplished. The silicon nitride is then etched from all non-frame areas, including all membrane areas, by reactive ion etching.

The frames are then formed by wet etching in an $\text{H}_2\text{O}_2/\text{NH}_3\text{OH}$ mixture [15] that selectively etches GaAs relative to AlGaAs. A brief non-selective etch (phosphoric acid/hydrogen peroxide/water) is then used to remove the AlGaAs etch stop. An additional lithography step and dry etch can be employed to expose metal beam leads overhanging the edges of the frames when such leads are desired.

The membranes with their associated RF structures and frames are now completely defined. The finished parts can be removed from the carrier wafer by dissolving the wax and any remaining photoresist in an appropriate solvent. The parts can be collected in a fine mesh placed in the bottom of the solvent vessel. No dicing or cleaving of the final parts is required. Process steps are shown in Fig. 2 and SEM micrographs of the finished parts appear in Fig. 3.

III. 2.5 THz MIXER

IIIa. Introduction and Concept:

The lowest order OH doublets at 2510 and 2514 GHz are strong tracers for the reaction rates of key ozone depleting cycles in the Earth's atmosphere. By a fortuitous coincidence of nature, a strong methanol laser line at 2522 GHz can be used as a pump source for heterodyning; producing IF's at 8 and 12 GHz. An O_2 line at 2502 GHz provides a convenient pressure (altitude pointing) calibration at an IF of 20 GHz. A receiver noise temperature of 20,000K single sideband (30K for receivers at both polarizations) provides enough sensitivity to allow daily global stratospheric maps of OH above 35 km and weekly zonal maps above 18 km from a satellite in polar orbit. These requirements are consistent with the performance that can be obtained from state-of-the-art room-temperature Schottky diode mixers.

Whisker-contacted corner cube mixers have been used at frequencies at and above 2.5 THz for many

years [16-19 for example]. Although the performance that has been reported [18], can be exceptionally good compared to mixers at other frequencies, as far as space-based remote sensing applications are concerned, the corner-cube suffers from three major drawbacks: (1) low reliability (anyone who has used one will attest to this), (2) poor beam quality and (3) extremely tight assembly tolerances that substantially affect RF performance and beam shape.

Recently, a group at Rutherford Appleton laboratory fabricated a waveguide-based 2.5 THz mixer with a novel "planar-whisker" contact [20]. The reported performance of this mixer was not quite as good as the better corner-cubes, but was very reasonable, and subsequent work has improved the noise temperature substantially [21]. Advantages of the RAL mixer include improved reliability (the planar whisker is more repeatable and reliable than its corner-cube counterpart) and in the improved efficiency obtained from single-mode waveguide-to-horn antennas. Members of the RAL team also proposed [22] a structure, which goes several steps further and integrates the semiconductor diode and whisker contact into a fully planar circuit that can be coupled to a photolithographically defined waveguide.

The technology presented in this paper has the same goals as the Rutherford Appleton work: to increase the reliability and performance of THz diode mixers relative to the traditional corner-cube mixers. We utilize the monolithic membrane diodes (MOMED's) described in the previous section, integrated into a mechanically machined waveguide circuit. This combination affords high reliability, solid performance, and ease of assembly.

IIIb. Mixer Design and Fabrication:

The mixer design is based upon a scaling of lower frequency single-ended mixer circuits with modifications that allow for relatively simple fabrication and assembly at 2.5 THz. Since the intended application is a space-based instrument, special consideration is given to device and circuit reliability and performance repeatability.

The mixer consists of five pieces: (1) the monolithic membrane diode (MOMED), which contains all RF filter circuitry, (2) an electroformed "button-mount" that houses the membrane and a single mode 2.5 THz signal waveguide and feed horn, (3) an interchangeable fixed depth "hobbed" backshort sec-

tion, (4) a fused quartz suspended-substrate IF transformer, and (5) a split-block housing that holds the RF and IF pieces as well as DC bias resistors and DC and IF connectors. A separate IF amplifier is required as well as an appropriate RF diplexer for LO injection.

The MOMED's unique bridge structure (Fig. 3) allows placement of the diode across the center of the broad wall of the 2.5 THz waveguide. Surrounding the diode on the membrane are low pass filters which both block RF propagation from the waveguide port and provide RF shorts at the waveguide walls. Unlike the configuration described in [2], the thin (36 μm wide, 600 μm long) membrane bridge is actually suspended along the centerline of a sealed single-mode transmission line cavity (60 wide x 40 μm high cross-section, metal on all sides) forming a 3 μm thick GaAs suspended stripline circuit. The membrane support frame lies outside the sealed cavity (active RF area) and is intended to have no effect on the signal coupling. A finite difference time domain (FDTD) analysis [23] of the filter is shown in Fig. 4. An interesting result of the analysis was the appearance, at the center of the stop band, of what we believe is a propagating ridge waveguide mode between the membrane and cavity side. This mode could only be reliably suppressed by reducing the height of the stripline cavity from 60 to <40 μm , hence the resulting asymmetric cross section.

The membrane thickness (3 μm) was chosen as a compromise between ease of fabrication (epitaxial growths of >4 μm are expensive) and mechanical robustness. Careful adjustment of the membrane layer thickness to avoid mechanical stress (a concern in silicon nitride membrane configurations) does not appear to be necessary. In our tests a membrane thickness of 3 μm gave sufficient robustness to a 600 μm long, 36 μm wide beam, for withstanding fairly relaxed handling procedures. No strain related bowing was visible, even after device and metal deposition. Membranes of 1.2 and 2 μm thickness with widths varying between 10 and 80 μm were also fabricated on test wafers and, although they survived routine handling and had no signs of mechanical stress, the thinner membrane structures were deemed a bit too fragile for the repeated handling expected in a flight program.

The length of the membrane bridge was chosen to be as short as possible and still accommodate sufficient high/low impedance filter sections for reasonable RF rejection. The membrane frame size was selected to

be large enough for handling, yet small enough to have a negligible effect at the highest IF frequency (21 GHz). The diode epitaxial layer properties and anode area were selected to minimize parasitic effects without compromising severely the diode non-linearity (ideality factor no higher than 1.5). Initial wafer variations included only anode area (.1x1 and .2x1 microns), anode finger shape (an S-bend was included in case stress on the membrane turned out to be a problem; it didn't) and required process variation bracketing. A membrane variation which included overhanging beam leads (for IF and DC bonding) was also included, but processing of the beam leads was not completed on the first device run.

Upon completion of the membrane fabrication process, the separated circuits are collected on filter paper, transferred en masse to a wafer holder and individually probed and sorted before being inserted into the mixer block. Device yield on the first quarter wafer run was fairly poor with only about 10% of the diodes surviving with good DC performance characteristics (series resistance below 20 ohms, leakage current below 5 microamps). Yields were limited by three problems. The photolithographically defined air-bridges need to be slightly altered on future runs. Also, the e-beam anode formation is quite difficult, and the first wafer's yield was particularly low in this step. Finally, device characteristics appear to have degraded through backside processing, particularly on the devices with smaller anodes. Improvements have been made in the backside process that should eliminate the last problem. A second quarter wafer is now in processing.

Mechanically, almost all the membrane structures survived intact and there is no observed strain or strain related problems (diodes that were processed to completion did not fail during storage or handling although their small area makes them more susceptible to damage from static discharge than our lower frequency diodes). Device reliability appears to be very high, although no Arrhenius tests have as yet been completed. Sample devices were thermally cycled from -50 to +150 C (10 cycles, 15 minute dwell) with no observed changes in their DC characteristics. One mounted device was also subjected to vibration (average 9.2 g's, 10 Hz to 2 kHz) with no mechanical problems. During device mounting, the membrane frames are picked up, dropped into place in the mixer block, glued with cyanoacrylic, probed and finally subjected to ultra-

sonic wire bonding (one bond on each side) while they are in place in the waveguide block, all with no apparent detrimental effects.

The RF coupling circuit, which provides signal and LO to the membrane diode, is formed in a standard copper electroforming operation. This electroformed "button mount" (Fig. 5.) contains a single mode 2.5 THz rectangular waveguide (nominally 100x50 microns), a tapered transition to circular waveguide and a scaled Pickett-Potter dual mode feed horn [24] (aluminum mandrel shown in Fig. 6).

Other than the small waveguide dimensions, no special requirements are placed on the fabrication at this point. Following electroforming, but while the aluminum mandrel still fills the waveguide cavity, the button mount is machined to final size (.187x.075"). A relief cavity to house the membrane frame is then milled into the copper and the suspended stripline filter cavity is machined across the button and through the center of the waveguide using a high speed diamond saw with a cubic boron nitride blade. The depth of the stripline cavity channel is set at this time to precisely locate the membrane bridge and frame below the surface of the button, at a depth determined by two support ledges that have been machined into the frame relief slot. These ledges catch, and support, the bottom of a membrane web left between two dog-ears on the sides of the membrane frame. Since the ledge references the membrane itself, it precisely positions the suspended stripline filter vertically in the enclosed cavity. After dicing the stripline slot, the aluminum mandrel is etched out of the copper button using NaOH.

The button mount is press fit into a brass split-block mount that also contains a much larger stripline cavity to house the IF transformer and the bias and IF connectors. Machining of this portion of the mixer block is straightforward.

In order to provide some degree of adjustable matching to the diode, a fixed depth backshort cavity, aligned with the 2.5 THz waveguide, is added over the top of the membrane. Since the membrane frame support ledges locate the membrane and the top of the frame below the top surface of the button mount, the waveguide and stripline cavity are completely sealed off by the backshort cavity block. The backshort cavity itself is easily formed using a hobbing technique to punch the rectangular hole to depths as great as several mils. A range of cavity depths is readily obtained by repeated "hobbing" to produce random depths and a few finishing strokes on some

fine lapping paper. Alignment of the blind waveguide in the backshort piece with the waveguide in the button mount is accomplished by picking up alignment holes in both parts under an optical microscope. The fixed backshort feature makes tuning rather time consuming, but assures extremely stable and repeatable measurements and requires no changes for flight implementation. Optimal cavity depth so far varies only by a few microns for different diodes of the same nominal anode size.

The final piece of the mixer block is the IF transformer which converts the expected diode output impedance of 200-250 ohms to 50 ohms over the required IF bandwidth of 7-21 GHz. In order to be mechanically and electrically compatible with the tiny membrane structure and at the same time provide a very high impedance at the output of the GaAs filter, a thin (125 μ m) fused quartz, suspended stripline transformer design was selected. The stripline cavity is sized to provide the 250-to-50 ohm impedance range and match (at the connector side) to a standard microstrip launcher. Due to some initial moding problems with the connector-to-stripline joint at 20 GHz, the original wide tab (0.050") launcher had to be replaced with a .020" wide tab launcher [25]. A through measurement on two back-to-back 200-to-50 ohm transformers is shown in Fig. 7.

Assembly of the mixer block is fairly simple and can usually be accomplished in less than an hour. The membrane device is carefully placed in position in the provided button cavity and checked for relative height with respect to the provided support ledges (usually not a problem, so long as no particulates have fallen onto the ledge). The frame is then held in place with a wafer probe while cyanoacrylic is generously applied to the frame edges. The quartz stripline is already glued in place at this time. Half mil wire bonds are now added from the frame across to the quartz stripline filter metal on one side, and to the continuation of the stripline channel slot on the far side of the button mount. Bonds are also added for the bias resistors and the tab launcher at this time. The backshort cavity is then lightly screwed in place and optically aligned before being locked down with a set screw on the top half of the split block. A photo of the assembled mixer (without the backshort cavity and with the top half removed) can be found as Fig. 8 and a close up of the membrane mounting is shown as Fig. 9.

IV. PERFORMANCE

Iva. Test System:

Accurate RF noise measurements at 2.5 THz are complicated by several factors: high mixer noise temperatures, variable atmospheric attenuation, poorly calibrated "absolute power" detectors, unavailability of matched attenuators, "gray body" loads, and imperfect Gaussian beams. The measurement test system used here to overcome these difficulties is shown schematically in Fig. 10. Local oscillator power is generated by a CO₂-pumped methanol gas laser with a maximum output power of more than 100 mW at 2522 GHz. A Martin-Puplett style wire grid diplexer is used to spatially combine the LO and signal beams. An off-axis ellipsoidal mirror matches the beam of the diplexer to that of the Pickett-Potter feed horn. The laser beam profile at 2.5 THz can be coarsely viewed with low thermal response liquid crystal paper, and, when the laser is properly tuned, appears to be circular with a single bright central spot. LO power measurement is provided by a "calibrated" Scientech multimode thermal detector and the numbers reported here should be taken with error bars of at least 3dB, due to beam mode and detector absorber non-idealities.

The noise temperatures are measured using the standard Y-factor technique on the full receiver only. A chopper switches the signal beam between a hot load (wedged Eccosorb CR110) and a cold load (Eccosorb AN74 flat sheet, soaked in liquid nitrogen, and held in the signal beam during the measurement. The assumed hot and cold load temperatures are 300 and 77K respectively, no corrections are made to account for mismatch or non-ideal Rayleigh-Jeans behavior. Note that incorporation of the more accurate Planck law would reduce the noise temperatures reported here by approximately 5%. A lock-in detector at the ≈ 100 Hz chopper frequency is used to extract a hot/cold load power output variation from a crystal diode detector. A correction factor of 0.45 is divided into the lock-in value to convert its RMS output to a peak-to-peak value (the chopper bowtie blade, radius 50 mm, produces a good approximation to a square wave as it switches the relatively small signal beam: waist radius of ≈ 4 mm). This peak-to-peak variation is then scaled by the DC average diode detector value to give the hot and cold powers needed for an accurate Y-factor measurement. This lock-in technique can be used to evaluate receivers with noise in excess of 500,000 K DSB.

For the results reported here, a broadband bias Tee [26] connects the mixer to a low-noise broadband IF amplifier [27]. The IF amplifier provides approximately 65 dB of gain over the frequency range 7 to 21 GHz, with noise at the low frequency end of ≈ 150 K, and at the high frequency end of ≈ 200 K. Coaxial filters [28] limit the detected bandwidth to ≈ 500 MHz about the desired center frequencies of 8.4, 12.8 and 20.4 GHz. Detected power is in the neighborhood of 10 microwatts. Front-end conversion loss is measured using a power meter to calibrate the response of the crystal diode detector, and extract the measured amplifier gain and filter loss (0.9 dB).

Mixer noise temperature can be extrapolated from the receiver measurements after separate IF amplifier calibration, but includes diplexer, atmospheric and horn coupling losses as well as any bias tee losses and IF impedance mismatch that may be present between the mixer output port and the amplifier. We can provide only approximate corrections for these losses until better calibration can be performed. They are distributed as follows: diplexer signal loss: 0.5 dB, mirror-to-horn coupling loss: 0.5 dB, IF mismatch loss: up to 3dB at 20 GHz based on relative IF measurements, atmospheric losses: 1 dB. More accurate values will be obtained in the future. For this paper, we will not attempt to calibrate out these losses, but will refer to "front-end" (rather than mixer) noise and loss as that belonging to all components forward of the IF amplifier.

During measurements, the mixer is current biased so that LO power fluctuations are compensated by a voltage change on the diode. We find that current bias (\approx curvature bias) makes the mixer relatively insensitive to changes of LO power. We observe nominally the same receiver noise temperature at fixed current when we alter the LO power by more than a factor of 5. The fluctuations visible on the graphs of noise temperature (Figs. 11-12) apparently arise from atmospheric fluctuations (variable water vapor content immediately in front of the cold load). In the near future, tests will be performed in vacuum to eliminate the effects of the atmosphere.

The entire RF noise test system is computer controlled and can be programmed to sweep bias current versus time to obtain the plots shown in the figures. Pumped and unpumped IV curves can also be generated (Fig. 11). Typically we operate with a lock-in time constant of 300 msec and 100 data points per curve.

IVb. Receiver/Mixer Noise:

The best measured receiver noise temperatures to date, using the test system described in the prior section, are given in Fig. 11. and are plotted against bias current flowing through the diode. The device which produced these results had a nominal area of $0.2 \times 1 \mu\text{m}^2$, a measured resistance of 16 ohms, an ideality factor of 1.53 and a saturation current of 3×10^{13} A. Smaller area devices have not yet yielded as good performance. A backshort depth between 12 and 25 μm consistently gave the best performance during tests of several different devices of varying resistance. Five devices have so far been measured and two have given performance similar to that shown in Fig 11. Fig. 11. also shows the dependence of receiver noise on LO power, with bias current again a fixed parameter. As can be seen from the figure, the current bias mitigates greatly the effect of LO power variation. In fact we were able to adequately pump the mixer with only 3 mW of measured LO power and could occasionally go as low as 2 mW without noticeably starving the diode. On the other extreme, pump power levels as high as 22 mW did not burn out the device and we could obtain essentially identical noise temperature vs. bias current curves for the two LO power extremes.

The extrapolated "front-end" noise, based upon a measured receiver conversion loss of 17 dB is shown in Fig. 12, again as a function of bias current at fixed LO power. All the data shown is at an IF of 8.4 GHz. At 12.8 GHz the receiver noise is within 5% that of 8.4 GHz, but at 20.4 GHz the noise performance is consistently a factor of two higher for all devices. We are not certain at this time of the origin of this degradation. One might focus on the IF chain, but as can be seen in Fig. 7, the IF transformer does not appear to account for the degradation, nor do the amplifier noise specifications.

We have not measured the mixer at any other LO frequency and the performance is sensitive to the backshort cavity depth. Changes of as little as 10 microns can result in changes of more than 50% in receiver noise. This is consistent with the sensitivity observed in lower frequency mixers that use full height waveguide.

So far we have measured only a small number of membrane devices and have not accumulated enough data to make any conclusions regarding the importance of the device DC parameters on RF performance. A large change in optimal backshort cavity depth was observed between the 0.1×1 and $0.2 \times 1 \mu\text{m}^2$ area diodes, with the smaller diodes requiring

more matching inductance (larger cavity depth), but a more detailed analysis on the full RF circuit has not yet been concluded. Only diodes with low leakage current and low series resistance (relative to those in the processed batch) have been measured so far and we cannot put any weights on the relative importance of these DC variables as yet. Further measurements on devices with different doping and epilayer profiles, anode areas and RF circuit configuration are clearly desirable. In the meantime we are preparing the existing mixer mount and membrane structure for use in space and are focussing more on reliability and system level parameters than performance at this time.

IVc. RF Beam Pattern:

As a final characterization measurement, we used the mixer as a direct detector to measure the beam pattern of the Pickett-Potter feed horn. The data is presented in Fig. 13. The laser beam quality allowed us to measure reliably only to the 10 dB level, but the beam widths at this and the 3dB point match those predicted in [24].

V. SUMMARY

A novel GaAs membrane diode circuit concept has been developed and demonstrated. The membrane fabrication process has been combined with our existing submillimeter-wave planar T-anode mesa Schottky diode process to design and fabricate a 2.5 THz waveguide mixer. Early measurements of mixer performance have shown the design to be competitive with alternative corner-cube and whisker contacted waveguide mixer concepts, although not as good as the best reported measurements in the literature. In addition, the required LO power is as low as 3mW (optimal) and 2 mW slightly starved. The membrane devices have proven to be both robust and reliable, having been taken through "shake and bake" at mil-spec levels. The waveguide block, although requiring careful machining and electroforming, is relatively simple to fabricate and assemble. The combination of the narrow membrane bridge circuit containing both the integrated planar diode and the RF filters, allows the implementation of sealed cavity single mode circuitry everywhere, even at wavelengths as short as 100 microns. The membrane fabrication process requires no post processing on the die as chemical etching replaces labor intensive dicing or scribe and break procedures. The lack of induced stress on the completed membrane makes it ideal

for circuits where long thin bridging is required. The circuit and device implementation demonstrated in this application can be employed for other submillimeter and millimeter wave components including multipliers or harmonic mixers (membrane couples to two different sized waveguides), heterodyne arrays (multiple membranes superimposed on a feed horn array), oscillators (cavity coupled membrane strip) or micromachined components (membranes used to span formed waveguides or cavities). The circuit described in this paper is being employed on a NASA flight mission and will undergo extensive lifetime and reliability screening before delivery of finished components.

VI. ACKNOWLEDGEMENTS

The authors would like to acknowledge the many valuable contributions of Pete Bruneau to the mixer block fabrication process. They would also like to thank John Oswald for help in setting up the FDTD analysis of the RF filters, Andrew Pease and Robert Lin for the device thermal cycling, Tracy Lee for the IF transformer processing and the remaining members of the SWAT (Submillimeter-Wave Advanced Technology) team for assorted technical support. Special acknowledgement is also due to Dr. Carl Kukkonen, Dr. Virendra Sarohia and Gary Lau at JPL for financial support of the program. This work was carried out at the California Institute of Technology Jet Propulsion Laboratory under contract with the National Aeronautics and Space Administration's Office of Advanced Concepts and Technology and the Earth Observing System Microwave Limb Sounder project office.

VII. REFERENCES

- [1]. G.V. Eleftheriades, W.Y. Ali-Ahmed and G.M. Rebeiz, "Progress in Integrated Circuit Horn Antennas for Receiver Applications: Part I and II," *Second International Symposium on Space THz Technology*, March 24-26, 1992, pp. 324-344.
- [2]. J.W. Kooi, M.S. Chan, P. Schaffer, B. Bumble, H.G. LeDuc, C.K. Walker and T.G. Phillips, "An 850 GHz Waveguide Receiver Using Tuned Nb SIS Tunnel Junction Fabricated on a 1 μm Si_3N_4 Membrane," *Seventh International Symposium on Space THz Technology*, March 12-14, 1996, pp. 86-102.
- [3]. G. de Lange, B. R. Jackson, A. Rahman, E. Duerr and Q. Hu, "Low-Noise Micromachined SIS Mixers for Millimeter-Wave Imaging Arrays," *Seventh International Symposium on Space THz Technology*, March 12-14, 1996, pp. 29-36.
- [4]. R.F. Drayton, C. Kidner, J. East and L.P.B. Katehi, "Micromachined Detector Mounts for Millimeter-Wave Applications," *Fifth International Symposium on Space THz Technology*, May 10-12, 1994, pp. 796-801.
- [5]. T. Weller, S. Robertson, L.P. Katehi and G.M. Rebeiz, "Millimeter and Submillimeter Wave Microshield Line Components," *Fifth International Symposium on Space THz Technology*, May 10-12, 1994, pp. 802-810.
- [6]. C.-Y. Chi and G.M. Rebeiz, "Planar microwave and millimeter-wave lumped elements and coupled-line filters using micromachining techniques," *IEEE Trans. Microwave Theory and Tech.*, vol. 43, no. 4, April 1995, pp. 730-38.
- [7]. Hjort, Klas, "Sacrificial Etching of III-V Compounds for Micromechanical Devices," *J. Micro-mech. Microeng.*, 6 (1996), pp. 370-375.
- [8]. Dehe, A., D. Pavlidis, K. Hong and H.L. Hartnagel, "InGaAs/InP Thermoelectric Infrared Sensor Utilizing Surface Bulk Micromachining Technology," *IEEE Trans. Electron Devices*, vol. 44, no. 7, July 1997, pp. 1052-1059.
- [9]. Uenishi, Yuji, H. Tanaka, and H. Ukita, "AlGaAs/GaAs Micromachining for Monolithic Integration of Micromechanical Structures with Laser Diodes," *IEICE Trans. Electron.*, E78-C, #2, 1995, pp. 139-145.
- [10]. Seassal, C., J.L. Leclerc, and P. Viktorovitch, "Fabrication of InP-based Freestanding Microstructures by Selective Surface Micromachining," *J. Micromech. Microeng.*, 6 (1996), pp. 261-265.
- [11]. C.I. Lin, A. Simon, M. Rodriguez-Gironies, H.L. Hartnagel, P. Zimmermann, R. Zimmerman, "Substrateless Schottky Diodes for THz Applications," to appear in *Proceedings of the Eighth International Symposium on Space THz Technology*, Cambridge, MA, April 1997.

- [12]. R.P. Smith, S.C. Martin, Moonil Kim, Jean Bruston, Dexter Humphrey, Neal Erickson, and P. H. Siegel, "Advances In Submillimeter Wave Semiconductor-Based Device Designs And Processes," to appear in *Eighth Int. Symposium on Space THz Technology*, Cambridge, MA, April 1997.
- [13]. T. Allen, M. Reddy, M.J.W. Rodwell, R.P. Smith, S.C. Martin, J. Liu and R. Muller, "Submicron Schottky-collector AlAs/GaAs resonant tunneling diode," *Proceedings Int. Electron Device Sym.*, Wash. D.C., Dec. 1993.
- [14]. R.E. Muller, S.C. Martin, and R.P. Smith, S.A. Allen, M. Reddy, U. Bhattacharya, and M.J.W. Rodwell, "Electron Beam Lithography for the Fabrication of Air-bridged, Submicron Schottky Collectors," *Journal of Vac. Sci. and Tech.*, Nov/Dec, 1994.
- [15]. W. Bishop, K. McKinney, R. Mattauch, T. Crowe, and G. Green, "A Novel Whiskerless Diode for Millimeter and Submillimeter Wave Applications," *1987 IEEE-MTT-S Digest*, June 1987, pp. 607-610.
- [16]. H. Krautle, E. Sauter and G.V. Schultz, Properties of a submillimetre mixer in an open structure configuration," *Infrared Physics*, vol. 18, 1978, pp. 705-712.
- [17]. J. Zmuidzinis, A.L. Betz and R.T. Boreiko, "A Corner-Reflector Mixer Mount for Far Infrared Wavelengths," *Infrared Physics*, vol. 29, no. 1, 1989, pp. 119-131.
- [18]. H.W. Hubers, T.W. Crowe, G. Lundershausen, W. C.B. Peatman and H.P. Roser, "Noise temperature and conversion losses of submicron GaAs Schottky-barrier diodes," *Fourth International Conference on Space THz Technology*, March 30-April 1, 1993, pp. 522-527.
- [19]. A.L. Betz and R.T. Boreiko, "A practical Schottky mixer for 5 THz," *Sixth International Symposium on Space THz Technology*, March 21-23, 1995, pp. 28-33.
- [20]. B.N. Ellison, B.J. Maddison, C.M. Mann, D.N. Matheson, M.L. Oldfield, S. Marazita, T. W. Crowe, P. Maaskant, W. M. Kelly, "First Results for a 2.5 THz Schottky Diode Waveguide Mixer," to appear in *Proceedings of the Eighth International Symposium on Space THz Technology*, Cambridge, MA, April 1997.
- [21]. Dr. Chris Mann, Rutherford Appleton Lab, private communication.
- [22]. S.W. Moon, C.M. Mann, B.J. Maddison, I.C.E. Turcu, R. Allot, S.E. Huq and N. Lisi, "Terahertz waveguide components fabricated using a 3D x-ray microfabrication technique," *Electronics Letters*, vol. 32, no. 19, 12 Sept. 1996, pp. 1794-1795.
- [23]. J.E. Oswald, P.H. Siegel and S. Ali, "Finite Difference Time Domain Analysis of Coplanar Transmission Line Circuits and a Post Gap Waveguide Mounting Structure," *Fifth International Conference on Space THz Technology*, Ann Arbor, Michigan, May 10-12, 1994.
- [24]. H.M. Pickett, J.C. Hardy and J. Farhoomand, "Characterization of a Dual Mode Horn for Submillimeter Wavelengths," *IEEE Trans. Microwave Theory and Techniques*, vol. MTT-32, no. 8, Aug. 1984, pp. 936-8.
- [25]. CDI part numbers 5753 CC or 5763 CC, available from Midwin and Olifson, 2400 Grand Ave., Long Beach, CA 90815.
- [26]. Wiltron model K250 bias Tee, Wiltron Co., 490 Jarvis Drive, Morgan Hill, CA 95037-2809
- [27]. Miteq model JSD2-00010, MITEQ, Inc., 100 Davids Drive, Hauppauge, NY 11788
- [28]. K&L Microwave, Inc., 408 Coles Circle, Salisbury, MD 21804.

FIGURES

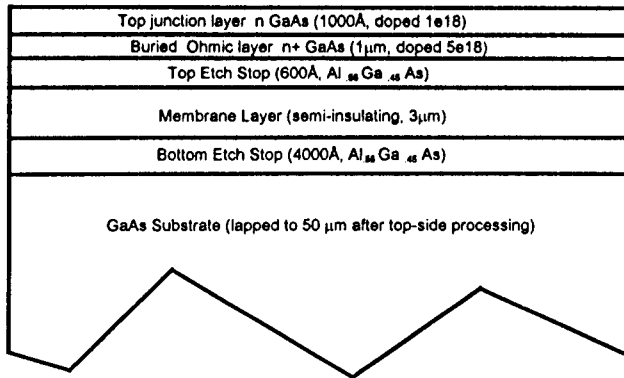
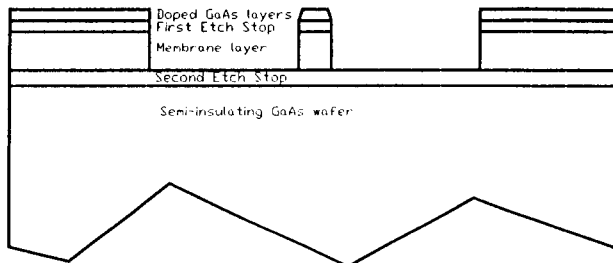
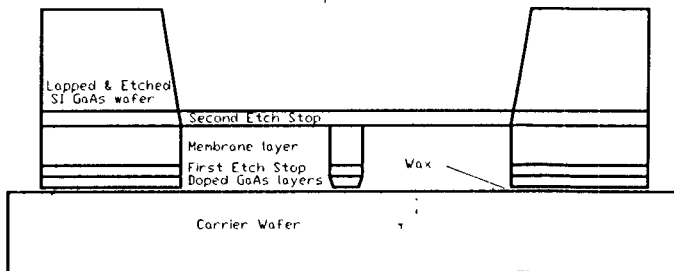


Fig. 1. Wafer profile for membrane and device/RF circuit definition. Layer pattern (from top): n doped GaAs, n+ GaAs, AlGaAs etch stop (device definition) followed by semi-insulating GaAs (membrane layer), AlGaAs etch stop and host wafer (used to form frames).

Processed GaAs Wafer: Devices on Top



Wafer Mounted Upside Down on Carrier



Free Membrane Device and Frame

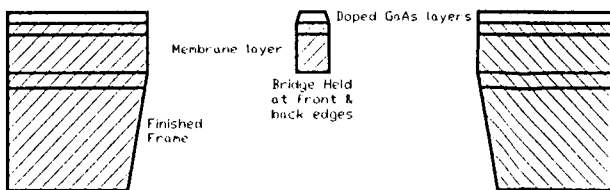


Fig. 2. Membrane fabrication steps. Top: Finished top-side wafer (with devices and RF circuitry) is etched down to lower etch stop, defining membrane region. Middle: Wafer is mounted upside down on carrier using low temperature wax. Wafer is thinned, frame is patterned and etched out to bottom of membrane. Lower: Etch stop is removed, wax is dissolved, individual membranes and frame float off carrier and are collected by filter or screen at bottom of beaker.

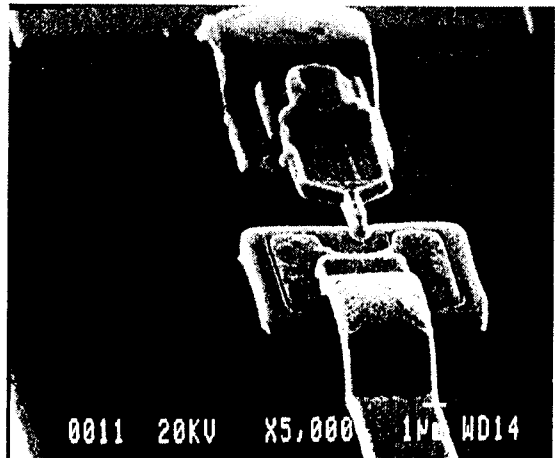
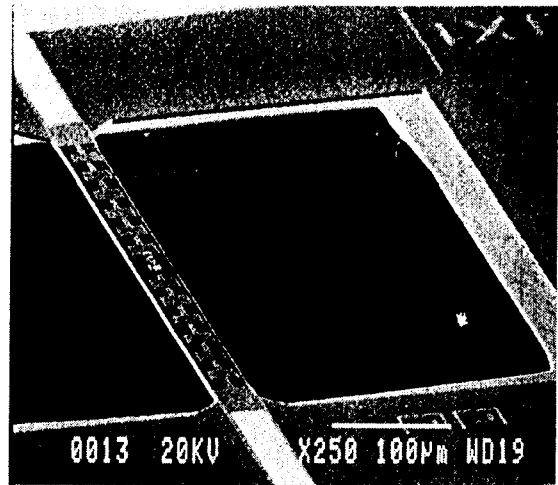
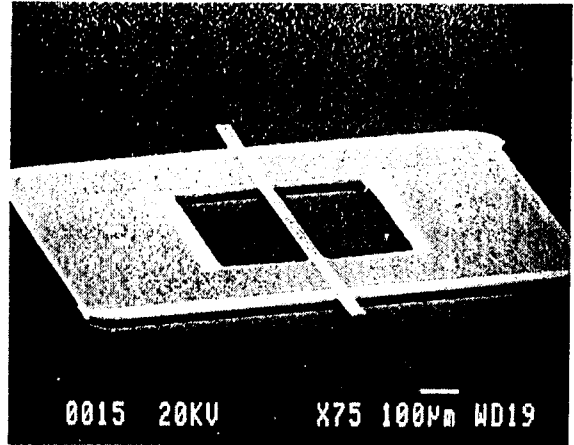


Fig. 3. SEM micrographs of completed membrane and frame with 2.5 THz Schottky diode and RF low-pass filter structure. Frame dimensions are 1x1.4 mm x 50 µm thick. Membrane is 36x600x3 µm thick.

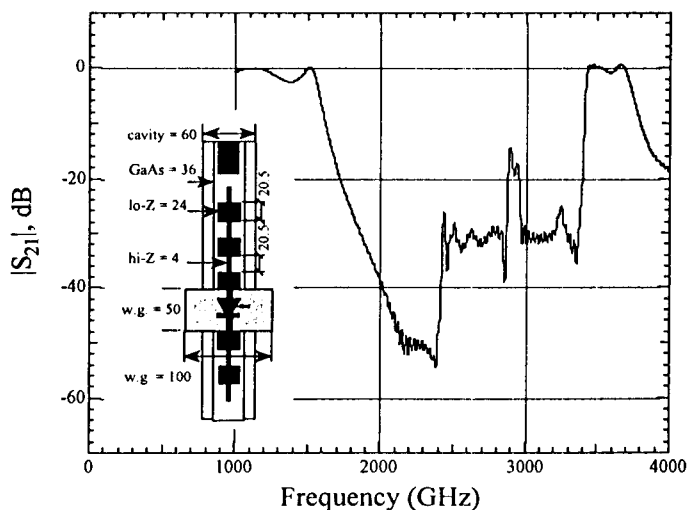


Fig. 4. Calculated finite-difference-time-domain performance of a 4-section RF choke with dimensions equal to those in the existing device. The inset shows a dimensioned (in μm) top view of the membrane strip as mounted. The cavity depth is $40\text{ }\mu\text{m}$. A more ideal configuration would utilize a $30\text{ }\mu\text{m}$ cavity depth and a $30\text{ }\mu\text{m}$ wide GaAs membrane strip, as asymmetries in the membrane mounting would be less likely to induce undesired mode propagation.

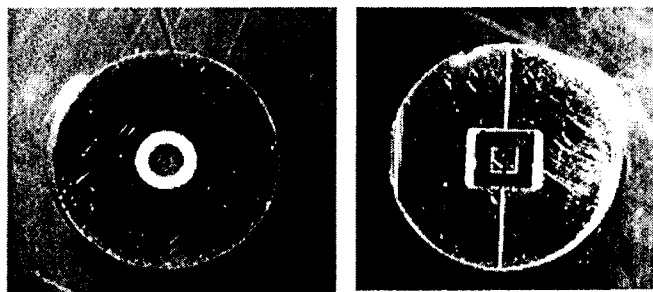


Fig. 5. 2.5 THz electroformed "button-mount" showing horn aperture on one side and 2.5 THz waveguide with inserted membrane mixer, MOMED, on the other.

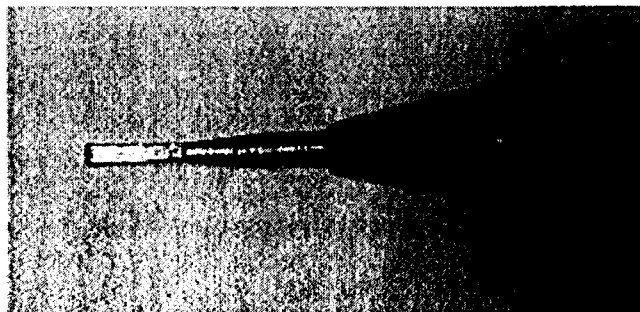


Fig. 6. 2.5 THz Pickett-Potter feed horn mandrel. Tip dimensions are $50 \times 100\text{ }\mu\text{m}$. Mandrel is etched away in NaOH after electroforming.

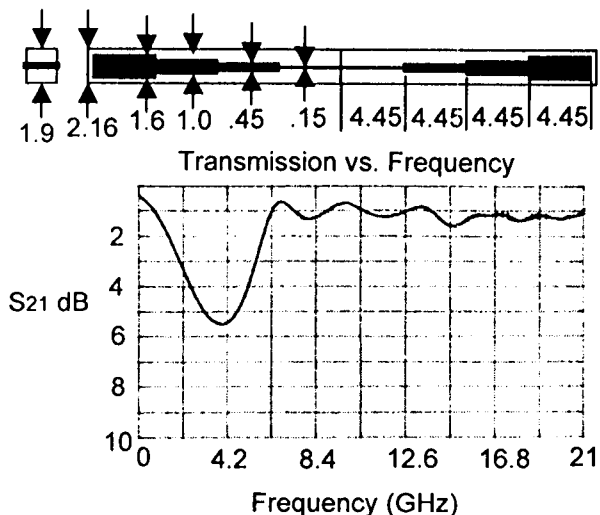


Fig. 7. Dimensioned diagram (in mm) and HP8510 plot of transmission loss for two back-to-back 7-21 GHz suspended-substrate IF transformers ($50\text{-}200\text{ }\Omega$). Quartz = $.15\text{ mm}$ thick, cavity = 1.9 mm square.

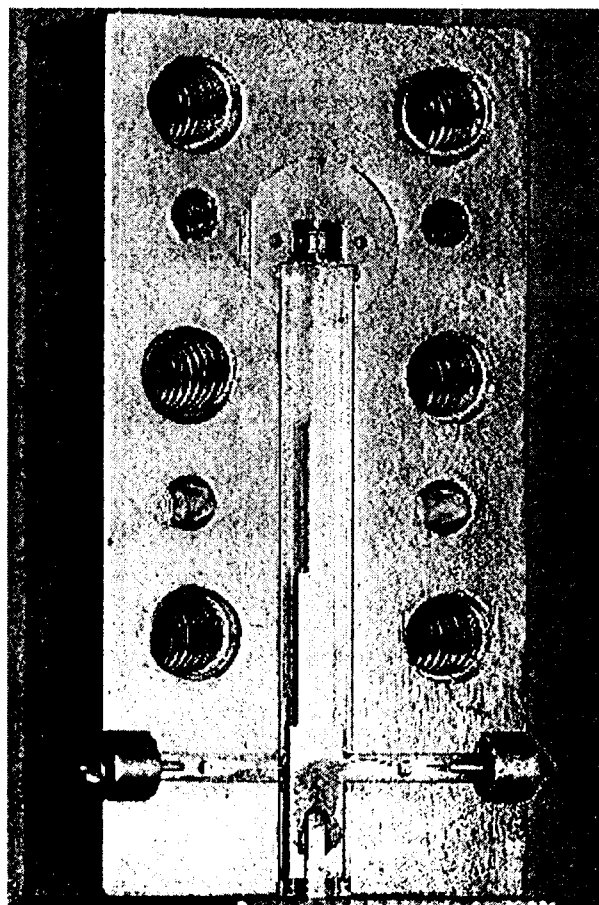


Fig. 8. Photo showing bottom half of complete 2.5 THz mixer block with RF membrane diode, quartz IF transformer and DC bias resistor and sensing taps. A backshort tuner cavity and top block seal the membrane and IF transformer cavities.

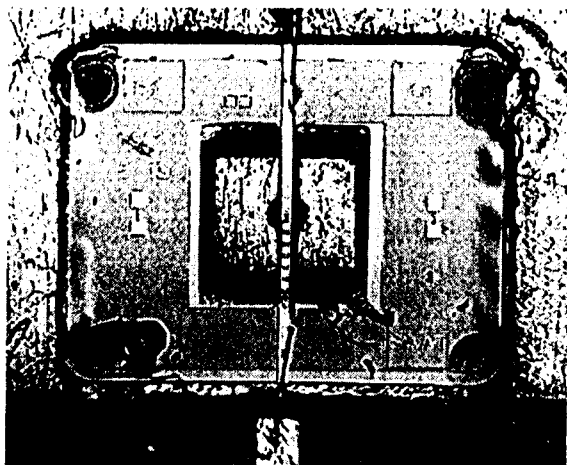


Fig. 9. Close up showing monolithic membrane mixer (MOMED) mounted in "button" with diode suspended across 2.5 THz waveguide (center), DC return (top) and IF transformer wire bond (bottom). RF test set schematic for 2.5 THz

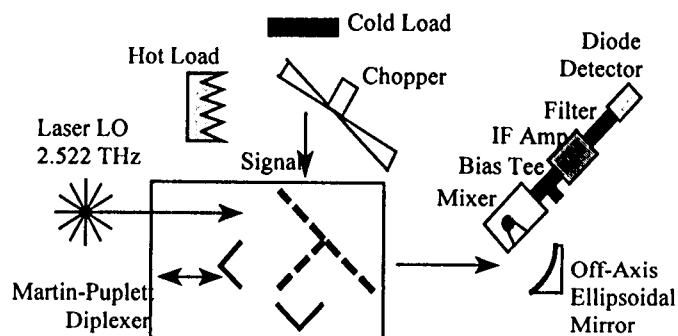


Fig. 10. Schematic of the RF test system used to collect the performance data given in this paper.

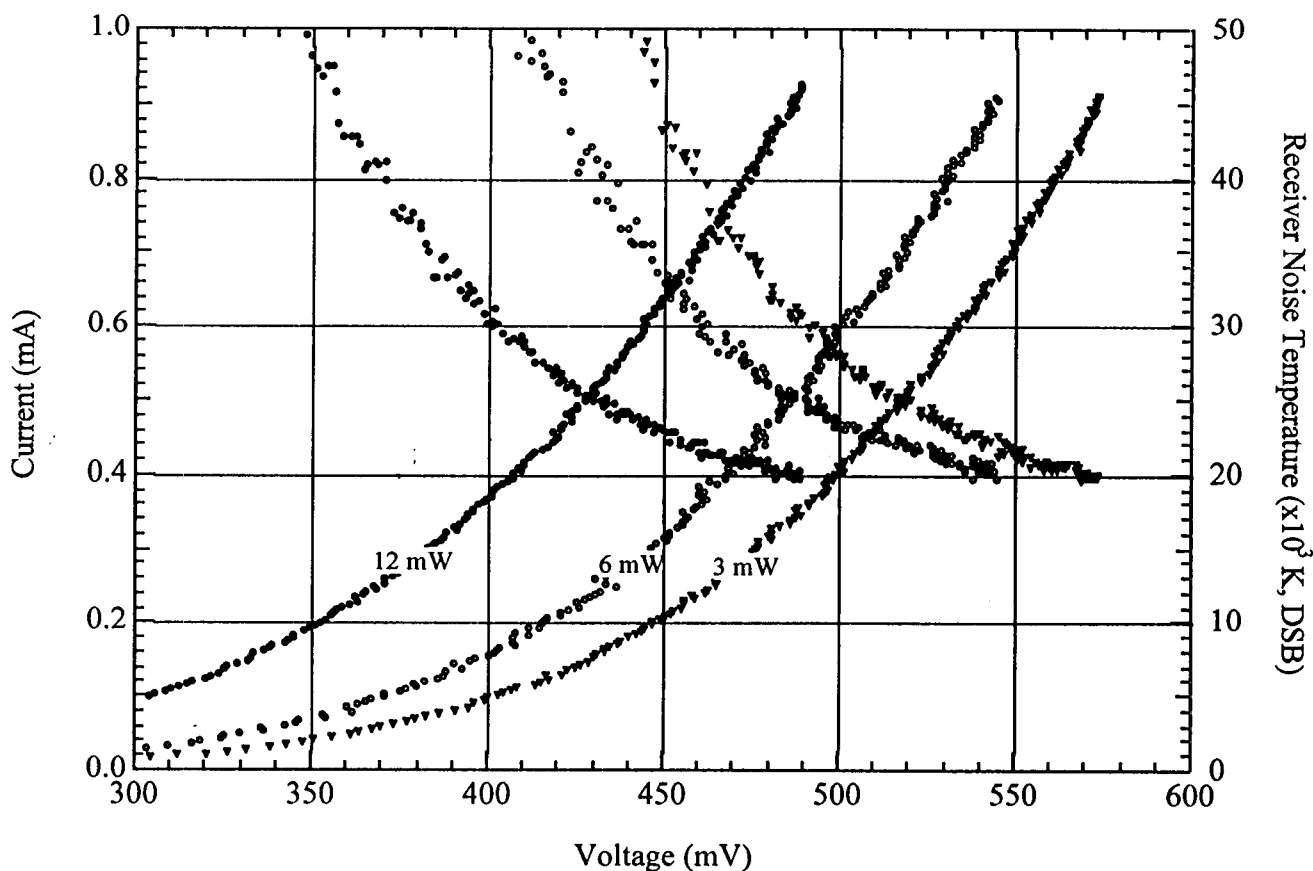


Fig. 11. Measured bias current and receiver noise temperature as a function of bias voltage for LO power levels of ≈ 12 , 6, and 3 mW (left-to-right). The bias current curves exhibit monotonic positive slope, noise temperature curves negative.

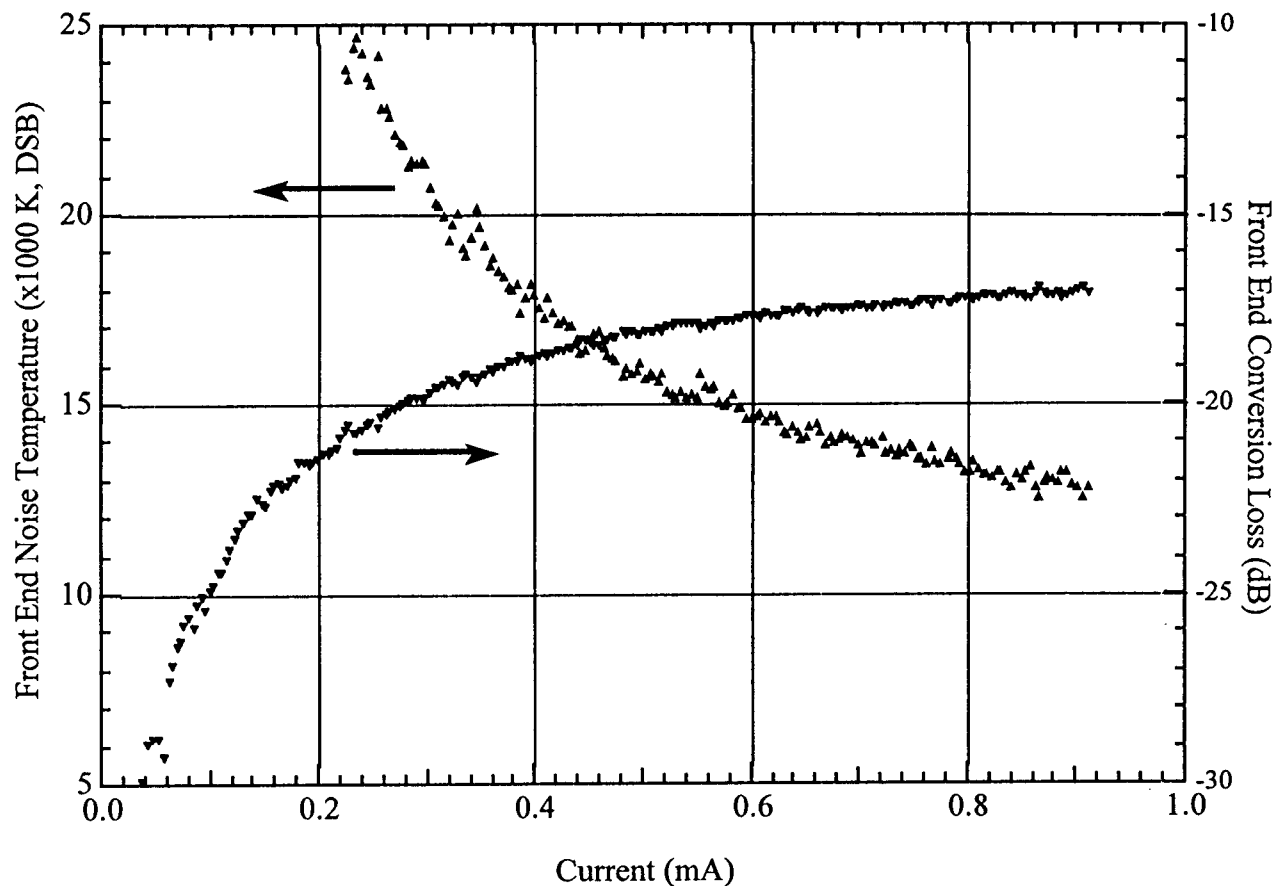


Fig. 12. Extrapolated “front-end” noise temperature and conversion loss. No corrections for diplexer, horn, air, IF mismatch, bias tee, or Rayleigh-Jeans approximation have been included. The minimum noise temperature is $\approx 12,500$ K, DSB, and the minimum conversion loss is ≈ 17 dB. When plotted against bias current as above, noise temperature and conversion loss curves overlap for LO powers between 3 mW and 22 mW.

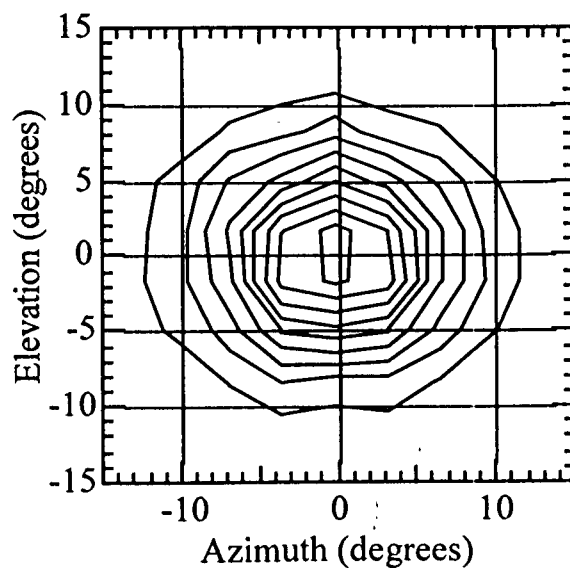


Fig. 13. Measured beam pattern of 2.5 THz Pickett-Potter feed horn using the LO pump laser as the RF source and the mixer as a direct detector. The contours are linearly spaced in 10% intervals (i.e., the outer contour has 0.1 times the signal strength of the peak).